esa ECOSPHERE

Calibrating and adjusting counts of harbor seals in a tidewater glacier fjord to estimate abundance and trends 1992 to 2017

JAMIE N. WOMBLE [1,†] JAY M. VER HOEF [2] SCOTT M. GENDE [1] AND ELIZABETH A. MATHEWS [3,4]

[1]National Park Service, Glacier Bay Field Station, 3100 National Park Road, Juneau, Alaska 99801 USA
[2]Marine Mammal Laboratory, NOAA Fisheries, Alaska Fisheries Science Center, 7600 Sand Point Way NE, Seattle, Washington 98115 USA
[3]Natural Sciences Department, University of Alaska Southeast, 11066 Auke Lake Way, Juneau, Alaska 99801 USA

Citation: Womble, J. N., J. M. Ver Hoef, S. M. Gende, and E. A. Mathews. 2020. Calibrating and adjusting counts of harbor seals in a tidewater glacier fjord to estimate abundance and trends 1992 to 2017. Ecosphere 11(4):e03111. 10.1002/ecs2.3111

Abstract. Long-term monitoring for understanding status and trend of species of conservation concern is undeniably valuable, yet monitoring methods often evolve over time due to the development of new technology, fluctuations in funding, logistical constraints, and innovations in sampling methods or analytical approaches. Consequently, valuable insights into annual or decadal-scale trends can be lost unless calibration between historical and current methods is developed. Glacier Bay National Park, in southeastern Alaska, hosts an important regional population of harbor seals, with the majority of seals pupping and molting on icebergs calved from a tidewater glacier in Johns Hopkins Inlet. Monitoring efforts to assess abundance and trends of harbor seals used counts of seals by shore-based observers from 1992 to 2002, but transitioned to aerial photographic surveys in 2007 through 2017. To produce a rigorous long-term evaluation of abundance and trends of harbor seals, we (1) conducted concurrent shore-based counts and aerial photographic surveys in 2007 and 2008; (2) developed an analytical calibration between the two monitoring methods; (3) developed a haul-out model to estimate the number of harbor seals in the water at the time of counts; and (4) estimated abundance and trends of harbor seals from 1992 to 2017 from the adjusted counts. Our calibration analysis revealed that during the pupping season in June, counts of harbor seals by observers from shore were consistently lower than counts from aerial surveys. During the molting season, counts by shore-based observers were only slightly less than aerial photographic surveys, and there was an interaction between survey method and season. After calibrating methods, we found important decadal-scale changes in trend. Over the 26-yr period (1992–2017), the estimated trend was negative; however, trends computed for rolling 10-yr time intervals showed steep and significant declines ending around 2011, with leveling off and possibly some subsequent recovery. The most recent shorter-term (2013–2017) trends are negative again, rivaling the steepest decreases over the 26-yr period. Our calibration between two monitoring methods improved continuity for long-term monitoring for a species of conservation concern by taking advantage of new sampling methods and innovations in analytical approaches.

Key words: abundance; Bayesian calibration; fjord; harbor seal; ice; long-term monitoring; *Phoca vitulina richardii;* pinniped; tidewater glacier; trend.

Received 6 August 2019; revised 1 November 2019; accepted 30 January 2020; final version received 7 March 2020. Corresponding Editor: Lucas N. Joppa.

[4]Present address: 1350 Yulupa Avenue Unit B, Santa Rosa, California 95405 USA.
† **E-mail**: Jamie_Womble@nps.gov

Introduction

Long-term monitoring is an unequivocally important tool for natural resource managers, particularly for entities focused on conserving species. However, monitoring methods often change over time due to different objectives, budgetary fluctuations, logistical constraints, and innovations in sampling methods or analytical approaches (Udevitz et al. 2001, Williams et al. 2017). The result is that inferences from long-term data and trends can be hindered, particularly for species such as marine mammals (Goodman, 2004, Baker et al. 2016, Boveng et al. 2018), where precise estimates of abundance collected over long time periods are necessary to detect even precipitous declines (Taylor et al. 2007). To improve the continuity of long-term monitoring and the multi-year and decadal-scale estimates of trend and comparison of abundance and inferences derived thereby, a calibration should accompany shifts in monitoring methods.

Some of the largest aggregations of harbor seals (*Phoca vitulina*) in the world occur seasonally in tidewater glacier fjords in southeastern and southcentral Alaska (Jansen et al. 2015), where seals use icebergs as a substrate for resting, pupping, molting, and avoiding predators. Harbor seals serve as an important cultural and subsistence food source for Alaska Natives (Crowell, 2016), play an important role in the marine ecosystem as both consumer and prey (Kiszka et al. 2015), and are a highly sought after viewing experience for visitors to Alaska, including those on cruise ships, which may disturb seals and potentially influence their energy budgets (Jansen et al. 2010, Young et al. 2014, Mathews et al. 2016). However, there is significant uncertainty related to the long-term viability of harbor seal populations that use tidewater glacier fjords because most of the ice sheets that feed tidewater glaciers in Alaska are thinning and retreating (Arendt et al. 2002, Larsen et al. 2007). Thus, in the context of understanding the implications of climate change, to meet legal mandates required under the U.S. Marine Mammal Protection Act, and for general management and conservation efforts, understanding long-term status and trend of harbor seals in fundamentally important.

Unfortunately, implementing and maintaining long-term monitoring to estimate the abundance and trend of harbor seals in tidewater glacier fjords is challenging due to the expansiveness and remote nature of these sites (Boveng et al. 2003, Bengtson et al. 2007). In addition, the distribution and number of seals in fjords is dynamic (Mathews and Kelly, 1996, Womble and Gende, 2013) and may change depending upon seal behavior, the availability and distribution of ice, and other environmental variables including prey distribution (Mathews and Pendleton, 2006, Womble et al. 2014, McNabb et al. 2016). Although harbor seals may travel widely during the post-breeding season, they exhibit a high degree of fidelity to tidewater glacier fjords during the pupping and molting seasons (Womble and Gende, 2013). Despite large aggregations of seals occurring at approximately 30 tidewater glacier fjords in Alaska, long-term monitoring has occurred at just two sites, Aialik Bay in Kenai Fjords National Park and Johns Hopkins Inlet in Glacier Bay National Park Alaska (Mathews and Pendleton, 2006, Womble et al. 2010, Hoover-Miller et al. 2011, Hoover-Miller and Armato, 2017), making the value of these sites and their related monitoring efforts, particularly important.

In Johns Hopkins Inlet in Glacier Bay National Park, consistent population monitoring of seals in the fjord began in 1992 using observers positioned at an elevated (~35 m above sea level) shore-based site. These surveys continued through 2002. Analysis of trend indicated a steep decline in the number of seals counted in the fjord, raising concern for this population (Mathews and Pendleton, 2006) and stimulating research aimed at identifying potential causes of the decline (Mathews and Adkison, 2010, Blundell et al. 2011, Hueffer et al. 2011, Womble and Gende, 2013, Young et al. 2014). However, to address issues with bias related to detection of seals on drifting icebergs from the low-angle shore-based observation site, aerial photographic methods were developed using a camera mounted in a fixed-winged aircraft to survey seals in the fjord (Mathews et al. 1997, Jansen et al. 2006, Bengtson et al. 2007). Beginning in 2007, there was a transition to aerial photographic surveys in Johns Hopkins Inlet for estimating abundance and trends of harbor seals

using new sampling methods and analytical approaches developed by Jansen et al. (2006) and Ver Hoef and Jansen (2015). The aerial photographic surveys are consistent with methods that are used to survey harbor seals at tidewater glacier fjords throughout Alaska and have the advantage of providing for greater spatial coverage of the fjord and producing a permanent record of seal distribution and ice habitat.

Our first objective was to calibrate harbor seal estimates between the two survey methods (counts by shore-based observers: 1992 to 2002 and aerial photographic surveys: 2007 to 2017), to allow for rigorous long-term trend and abundance estimates. Our results depended on simultaneous shore-based and aerial photographic surveys (2007, 2008) that provided data for the analytical calibration. Our second objective was to develop a haul-out model to estimate the proportion of seals in the water at the time of surveys, which was necessary to adjust the counts to total abundance. Finally, from the calibration and haul-out models that were used to generate abundance estimates, our goal was to assess trend across the 26-yr time period from 1992 to 2017. We used a Bayesian hierarchical model to combine the three disparate data sources (shore-based counts, aerial surveys, and haul-out data) and properly account for uncertainty when combining the models. The development of a calibration between the two monitoring methods, and subsequent adjustment by the haul-out model, allowed for improved continuity in long-term monitoring of harbor seals, a species of conservation concern, while taking advantage of advances in sampling methods and innovations in analytical approaches.

Methods

Study area

Johns Hopkins Inlet (58°50.896′ N, −137°06.121′ W) (Fig. 1) is an expansive (12 km long × 3 km wide) tidewater glacier fjord in the upper West Arm in Glacier Bay National Park, a Biosphere Reserve, and World Heritage Site encompassing over 600,000 acres (242,811 ha) of marine waters in southeastern Alaska. Harbor seals seasonally aggregate in Johns Hopkins Inlet to rest, pup, and molt on icebergs that emanate from two advancing tidewater glaciers, the Johns Hopkins (250 km^2), and the Gilman (25 km^2) glaciers, which extend from the Fairweather Mountain Range. After undergoing a retreat that began at the end of the 19th century, the Johns Hopkins Glacier has advanced nearly 2 km since the mid-20th century, and is one of the few advancing tidewater glaciers in Alaska (McNabb et al. 2015).

To develop a calibration between the two monitoring methods, we conducted shore-based counts and aerial photographic surveys of harbor seals in Johns Hopkins Inlet simultaneously during the pupping period in June (2007: 4 = surveys; 2008: 2 = surveys) and during the molting period in August (2007: 4 = surveys; 2008: 3 = surveys). Each monitoring method is described in detail below.

Shore-based counts by observers (1992–2002; 2007–2008)

Between 1992 to 2002 and 2007 to 2008, the numbers of seals on icebergs in Johns Hopkins Inlet were counted from an elevated observation site on shore (~35 m above sea level) by a pair of trained observers (Mathews and Pendleton, 2006, Womble et al. 2010). Paired counts were conducted using tripod-mounted 20 × 60 binoculars (Zeiss, Oberkochen, Germany), 2–3 times daily during survey periods in June and August. During the pupping period (June), seals were classified as either pups or nonpups, whereas all seals were classified as nonpups during the molting period in August owing to the difficulty in distinguishing pups and juveniles at a distance. Due to the expansive area of Johns Hopkins Inlet, pups at a distance may have been undetected (e.g., obscured by their mother or a piece of ice) or misclassified, and thus were likely to be underestimated. Therefore, in addition to counting the total number of pups, the proportion of pups from counts of 100 nearby seals were conducted multiple times throughout the day. Detailed methods of the shore-based counts can be found in Mathews and Pendleton (2006).

Aerial photographic surveys (2007–2017)

From 2007 to 2017, aerial photographic surveys of harbor seals in Johns Hopkins Inlet were conducted during the pupping period in June (n = 41 surveys) and during the molting period in August and September (n = 37 surveys)

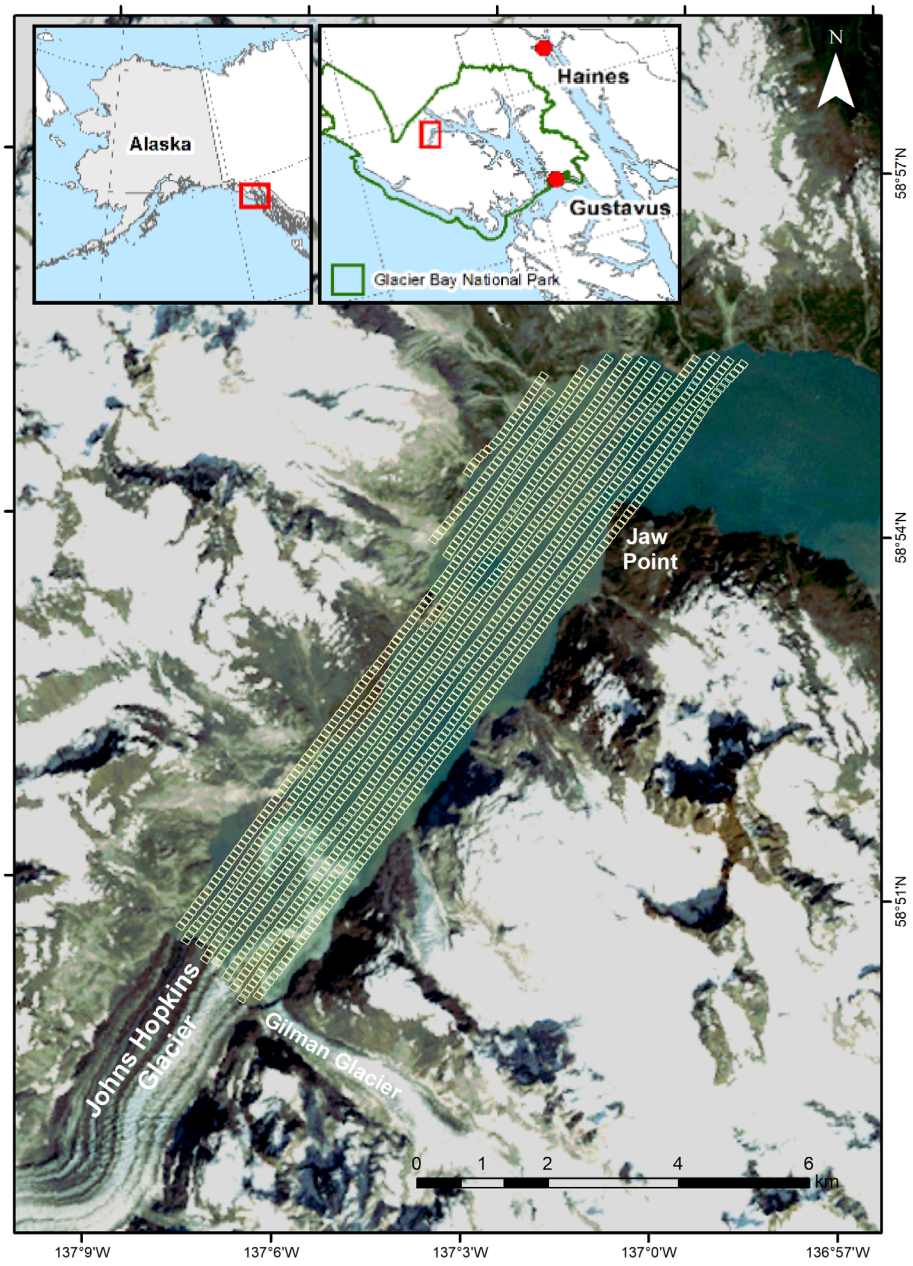

Fig. 1. Study area in Johns Hopkins Inlet in Glacier Bay National Park, southeastern Alaska. Light yellow boxes show footprints of aerial photographs along transects for one example survey.

(Table 1). Surveys were conducted between 1200 and 1700 Alaska Daylight Time, as higher counts of seals typically occur one to four hours after solar noon (Mathews and Pendleton, 2006).

Aerial photographic surveys were conducted from a de Havilland Canada DHC-2 Beaver single-engine high-winged aircraft (Ward Air Inc., Juneau, Alaska) following methods developed by Jansen et al. (2006) and Ver Hoef and Jansen (2015). The aircraft was flown at ca. 304 meters and ca. 90–95 kts along 12 established transects (Fig. 1). The transects were programmed into the navigation system (Chelton Flight Systems, Boise, Idaho) of the aircraft which created a 3D

Table 1. Dates of aerial photographic surveys (n = 78) in Johns Hopkins Inlet during the pupping period in June and the molting period in August and September from 2007 through 2017.

Year	June	August–September	Total Surveys
2007	18, 19, 20, 21	13, 15, 17, 22	8
2008	25, 29	11, 14, 15, 17	6
2009	20, 21, 23, 30	10, 12	6
2010	14, 15, 16, 17	13, 14, 16	7
2011	12, 13, 21, 22	8, 25	6
2012	12, 13, 20, 23	10, 14, 15, 16	8
2013	14, 19, 20, 21	13, 14, 15, 20	8
2014	19, 26, 27, 28	2, 3, 23	7
2015	12, 13, 19, 20	14, 20, 25, 26	8
2016	14, 16, 17	17, 20, 21, 28	7
2017	21, 22, 23, 27	29, 3, 5	7
n = 11	n = 41	n = 37	n = 78

image of each transect that the pilot used to maintain position and altitude. Transects were spaced 200 m apart, oriented perpendicular to the terminus of the Johns Hopkins Glacier, and spanned the length of the fjord from the terminus of the glacier to the opposite end of the fjord. The area along the transects encompassed an area of approximately 10.8 km^2 or approximately 48% of the 22.5 km^2 water's area of Johns Hopkins Inlet. An aerial survey of Johns Hopkins Inlet took approximately 1 h to complete.

During the aerial surveys, non-overlapping digital photographic images were taken directly under the plane using a vertically aimed digital single-lens reflex (DSLR) camera (Nikon D2X, 12.4 megapixel; Shinagawa, Tokyo, Japan) with a 60-mm focal length lens (Nikon AF Micro-NIKKOR, 2.8D). The camera was attached to a tripod head and mounted to a plywood platform that was secured in the belly porthole of the aircraft. The camera captured an image every 2 s, using a digital timer (Nikon MC36) operated by an observer. The firing rate and spacing of the transects allowed for a gap between images of 15 m end-to-end and 70 m side-to-side to ensure that images were separated from one another and so seals were only sampled once. Each digital photograph (3216 times × 2136 pixel JPEGS) covered approximately 80 × 120 m at the surface of the water with ca. 3.7-cm pixel resolution. Approximately 1200 digital images were taken during each survey. An onboard global positioning system (Garmin 76 CSX) was used to record the trackline and position of the plane along the transects at 2-second intervals. Aerial surveys were conducted under NOAA Fisheries Marine Mammal Protection Act (MMPA) permit numbers 358-1787-00, 358-1787-01, 358-1787-02, and 16094-02.

Post-processing of aerial digital imagery

The latitude, longitude, and altitude from the trackline were written to the EXIF headers of each digital image using RoboGEO V6.3 (Pretek, Incorporated, Christian, Tennessee, USA). Images from each survey were embedded as a raster layer in an ArcGIS project using ArcGIS (ESRI, version 9.3 and 10.1) and R (R Core Team 2017). Each photograph was scanned by a trained observer using digital photographic software (ACDSEE Pro 4), and each seal was marked as a point feature in an ArcGIS shape file.

After all seals were marked, "footprints" delineating the extent of each image were generated as polygons in a separate shape file. The point locations for seals were summed within each image and assigned to the centroid of each photo and exported as shape files for statistical analysis. The spatial extent of each survey was delineated by creating a polygon that was bounded by (1) the coastline of Johns Hopkins Inlet and (2) the terminus of the glacier. Shape files for pups and nonpups were generated for surveys in June, whereas only shape files for nonpups were generated for surveys in August and September.

Estimates from aerial surveys

Counts from photographs taken during aerial photographic surveys (Fig. 1) are specifically designed to have incomplete coverage, so represent only a portion of the seals hauled out on ice available for detection. Using the above described shape files of seal counts and distribution, we obtained estimates of the number of seals hauled out using the method of Ver Hoef and Jansen (2015), which included estimated standard errors.

Data for haul-out model

Counts of seals by shore-based observers and aerial photographic surveys do not account for the proportion of seals at sea and not visible to

be counted during surveys. Thus, data were collected by satellite-linked transmitters attached to harbor seals to estimate the proportion of time that seals spend in the water, which is necessary to develop a haul-out model to adjust counts of seals to estimate abundance.

Subadult and adult harbor seals (n = 25) (Table 2) were captured and fitted with satellite-linked transmitters during on-going research by Alaska Fisheries Science Center of NOAA Fisheries, Alaska Department of Fish and Game, and the National Park Service (Womble and Gende, 2013). One or two transmitters were deployed on each seal prior to release. SPLASH or SPOT tags (Wildlife Computers, Redmond, Washington, USA) were attached to the pelage on the head or back with fast-setting adhesive. Specially designed SPOT tags (Wildlife Computers) were attached to the inter-digital webbing of the rear flipper with screws and two mounting holes. When appropriate, given proper considerations of animal welfare, both device types were attached to each seal. The flipper-mounted satellite-linked transmitters (SPOT) remain attached during the molting period, whereas the adhesive mounted devices fall off when the seal sheds its coat of hair during the annual molt.

Location data were obtained via the Argos Data Collection and Location System operated by Service Argos (Collecte Localisation Satellite, CLS America, Inc., Largo, Maryland, USA). The satellite-linked transmitter detects contact with saline water many times per second and haul-out behavior summaries were sent via satellite. To conserve bandwidth for satellite transmission, the on-board data were summarized, per hour, into the proportion of time that the tag was dry. To further save bandwidth, these proportions, h, were put into categories with the following cut-points, {0, 0.05, 0.15, 0.25, 0.35, 0.45, 0.55, 0.65, 0.75, 0.85, 0.95, 1.00}, inclusive of hours that were all 0's, and those that were all 1's. Despite these features for reducing bandwidth, transmission of a complete haul-out behavior record for the duration of a deployment is rare and there are often periods of missing data. For building haul-

Table 2. Harbor seals that were instrumented with satellite-linked transmitters at glacial ice sites in Johns Hopkins Inlet and Endicott Arm in southeastern Alaska.

Animal ID	Capture Date	Sex	Age	Capture Location
PV2006-0113	9/6/2006	Female	Subadult	Johns Hopkins Inlet
PV2006-0114	9/6/2006	Female	Subadult	Johns Hopkins Inlet
PV2006-0115	9/11/2006	Female	Adult	Johns Hopkins Inlet
PV2006-0116	9/11/2008	Female	Adult	Johns Hopkins Inlet
PV2006-0117	9/13/2008	Female	Subadult	Johns Hopkins Inlet
PV2008-9002	6/26/2008	Female	Adult	Endicott Arm
PV2008-9005	6/28/2008	Female	Adult	Endicott Arm
PV2008-9006	6/28/2008	Female	Adult	Endicott Arm
PV2008-9008	6/28/2008	Female	Adult	Endicott Arm
PV2008-9012	6/30/2008	Female	Adult	Endicott Arm
PV2008-9011	6/30/2008	Female	Adult	Endicott Arm
PV2008-9013	7/1/2008	Female	Adult	Endicott Arm
PV2008-9015	7/1/2008	Male	Adult	Endicott Arm
PV2008-9020	9/12/2008	Male	Adult	Johns Hopkins Inlet
PV2008-9021	9/12/2008	Female	Adult	Johns Hopkins Inlet
PV2008-9023	9/13/2008	Male	Adult	Johns Hopkins Inlet
PV2008-9026	9/15/2008	Male	Subadult	Johns Hopkins Inlet
PV2009-9010	5/7/2009	Male	Subadult	Endicott Arm
PV2009-9011	5/7/2009	Male	Subadult	Endicott Arm
PV2009-9017	7/4/2009	Female	Adult	Endicott Arm
PV2009-9014	7/5/2009	Female	Adult	Endicott Arm
PV2009-9015	7/5/2009	Female	Adult	Endicott Arm
PV2009-9020	7/6/2009	Female	Adult	Endicott Arm
PV2009-9019	7/6/2009	Male	Adult	Endicott Arm
PV2009-9022	7/8/2009	Female	Adult	Endicott Arm

Note: Data from satellite-linked transmitters were used to develop haul-out model.

out models, the mid-points of each category were used as observed data, so $h \in \equiv \{0, 0.025, 0.1, 0.2, 0.3, 0.4, 0.5, 0.6, 0.7, 0.8, 0.9, 0.975, 1\}$.

Glacial fjords in Alaska that are used by harbor seals were delineated by polygons. The locations of seals from the satellite-linked transmitters were mapped in relation to the polygons. Haul-out locations of seals that were in, or nearer to a glacial polygon than any other terrestrial habitat, were included in the model. There were 9463 records of hourly haul-out proportion from 25 seals from 16 July to 30 September from 2006 to 2009 (Table 2) that were associated with glacial polygons. Haulout records were from Glacier Bay (Johns Hopkins Inlet, $n = 2560$; Tarr Inlet, $n = 96$) and two sites located approximately 200 km southeast of Glacier Bay (Endicott Arm, $n = 6447$; and Tracy Arm, $n = 360$). All count models, as described next, adjusted counts to 15 August to standardize abundance estimation. We restricted our haul-out analysis to the period from 16 July to 30 September, which allowed sufficient data before and after 15 August, to model a day-of-year effect in haul out during the molting period, and to estimate a haul-out inflation multiplier specific to 15 August for the adjusted counts.

Count models

We modeled raw counts, and estimates from aerial surveys, with lognormal distributions. If X is a normal random variable with mean α and variance σ^2, $X : N(\alpha, \sigma^2)$, then $Y = e^X$ is a lognormal random variable, $Y : LN(\alpha, \sigma^2)$ with.

$$E(Y) = \mu = e^{\alpha+\sigma^2/2} \tag{1}$$

and

$$\text{var}(Y) = e^{2\alpha+\sigma^2}\left(e^{\sigma^2} - 1\right) = \mu^2\nu^2 \tag{2}$$

where $\nu = \sqrt{e^{\sigma^2} - 1}$. Notice that ν is the coefficient of variation (CV), $\nu = \sqrt{\text{var}(Y)}/\mu$. The approach that we will take is to let $\log(\mu) = \mathbf{X\beta}$, where $\mathbf{X}$ is a design matrix of observed covariate values and $\boldsymbol{\beta}$ is a vector of regression coefficients. In this formulation, the quantity $\sigma^2/2$ will be absorbed into the overall mean, β_0, in the vector $\boldsymbol{\beta}$. This is an attractive feature. It is well known (Beauchamp and Olson, 1973) that after modeling log-transformed data, let the fitted mean be $\hat{\alpha}$, then the fitted mean back on the exponentiated scale requires a bias correction of $\exp(\hat{\alpha} + \hat{\sigma}^2/2)$, where $\hat{\sigma}^2$ is the estimated error variance. In our formulation, $\sigma^2/2$ is already absorbed into the mean. Another attractive feature of the μ, ν parameterization is that it allows the mean to be modeled separately from the coefficient of variation. Surveys of natural resources and many other disciplines often express uncertainty as CVs because we often expect the variance to increase with the mean, so evaluation of survey methods is revealed more clearly using CVs. We used $Y \sim \mathcal{L}(\mu, \nu)$ to denote the lognormal distribution under the parameterization given in Eqs. 1 and 2.

We chose the lognormal distribution because it was useful for modeling our abundance estimates. The abundance estimates came as two primary types: counts from shore-based surveys and estimated abundance from aerial surveys. The lognormal model kept all abundances greater than zero and had a separate variance parameter (CV) that allowed for overdispersed count data, and the CV parameter allowed us to directly use estimated CVs from aerial surveys.

We had six kinds of count data: shore-based counts of both pups and nonpups during pupping season, aerial surveys of pups and nonpups during pupping season, and both shore-based counts and aerial surveys of nonpups during molting season. Shore-based counts were used exclusively from 1992 to 2002, and aerial surveys started in 2007 through 2017. For two years, 2007 and 2008, both shore-based and aerial surveys were used to allow for a calibration due to the change in method. A linear model was used to examine relationships between shore-based vs. aerial surveys and pupping vs. molting estimates, and also account for having identifiable pups during pupping counts, but contained in the nonpups counts during molting. We describe the notation and linear model next.

We use i to denote year, $t_j; j \in \{p, m\}$ for the tth day-of-year divided into the early summer (mostly June) pupping period, where $j = p$ indicates pupping season, and the August molting period, where $j = m$ indicates the molting period. We will let r indicate replicates within day, and $k \in \{g, a\}$ for survey method as shore-based counts ($k = g$) or aerial surveys ($k = a$). Let $\ell = u$ indicate a pup count, and $\ell = n$ indicate a count of nonpups. Then, let $Y_{j,k,\ell}(i, t_j, r)$ be the count of pups ($\ell = u$) or nonpups ($\ell = n$) for survey type

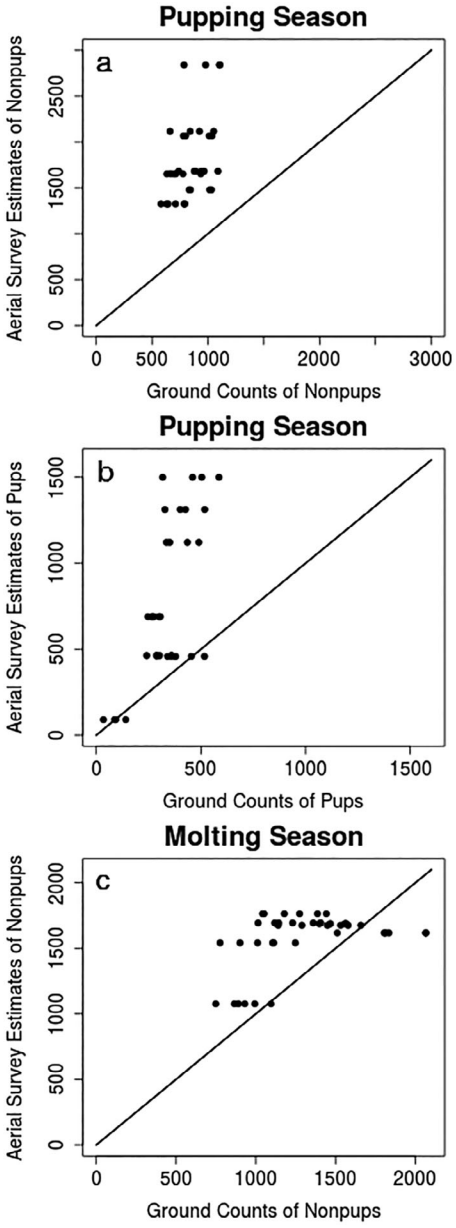

Fig. 2. Scatter plots of shore-based counts and aerial survey estimates on dates that were common to both during the pupping season for nonpups (a) and pups (b) and during the molting season for nonpups (c). Note that most days had several shore-based counts, but only one value per day for aerial surveys.

k, in year i on day t of season j, and the rth daily replicate. Note that $Y_{m,k,u}(i,t_j,r)$ does not exist for either $k=g$ nor $k=a$. The linear model for the mean, on the log scale, for pups and nonpups, for both shore-based and aerial surveys, during both pupping season and molting season, for each day and for each year, is.

$$\log\left(\mu_{j,k,\ell}(i,t_j)\right) = \eta + \xi_j + \tau_k + \xi\tau_{j,k} + \xi\pi_{j,\ell} + N_i + Z_j(i,t_j) \quad (3)$$

where η is an overall mean, ξ_j is an effect for surveys in the pupping or molting period, τ_k is an effect for survey method being shore-based count or aerial survey, $\xi\tau_{j,k}$ is a survey method by survey period interaction, $\xi\pi_{k,\ell}$ is an interaction term for pup versus nonpup counts by survey period, N_i is a zero-mean, temporally autocorrelated random effect for year, t_j is the day of year index, which has been set so that May 30 is $t_p=1$ for surveys during pupping period, and August 2 is $t_m=1$ for molting period, and $Z_j(i,t_j)$ is a zero-mean temporally autocorrelated random effect for days within year in survey period j, which are assumed independent among years and periods.

For identifiability, we let $\xi_m=\tau_a=0$, so these effects are nonzero during pupping period and for shore-based counts, respectively. The interaction term, $\xi\tau_{j,k}$, is nonzero only for shore-based counts during the pupping period. The interaction term, $\xi\pi_{k,\ell}$, is only nonzero value for $j=p$ and $\ell=u$, and because there is no main effect for π, we have effectively accounted for the fact that pups are only counted during the pupping period. For the temporally autocorrelated models, we let N_i follow an AR1 model, and we denote its conditional variance as $\sigma_N^2>0$ and autocorrelation parameter as $0\le\phi\le1$; that is,

$$N_i = \phi N_{i-1} + \delta_N W_i, \quad (4)$$

where $\{W_i\}$ are standard normal random variables and N_1 is 0. We let $Z_p(i,t_j)$ also follow an AR1 model, with a separate variance and autocorrelation for each survey period $j\in\{p,m\}$, denoted as δ_j^2 and autocorrelation parameter ω_j; that is, for a given year i,

$$Z_j(i,t_j) = \omega_j Z_j(i,t_j-1) + \delta_j W_j(i,t_j) \quad (5)$$

where $\{W_j(i,t_j)\}$ are standard normal random variables that are independent for all i,j, $Z_j(i,1)$ is 0, and all $Z_j(i,t_j)$ are independent across years. Note that while these variables are considered independent among years, we assume the autocorrelation parameters are constant among them.

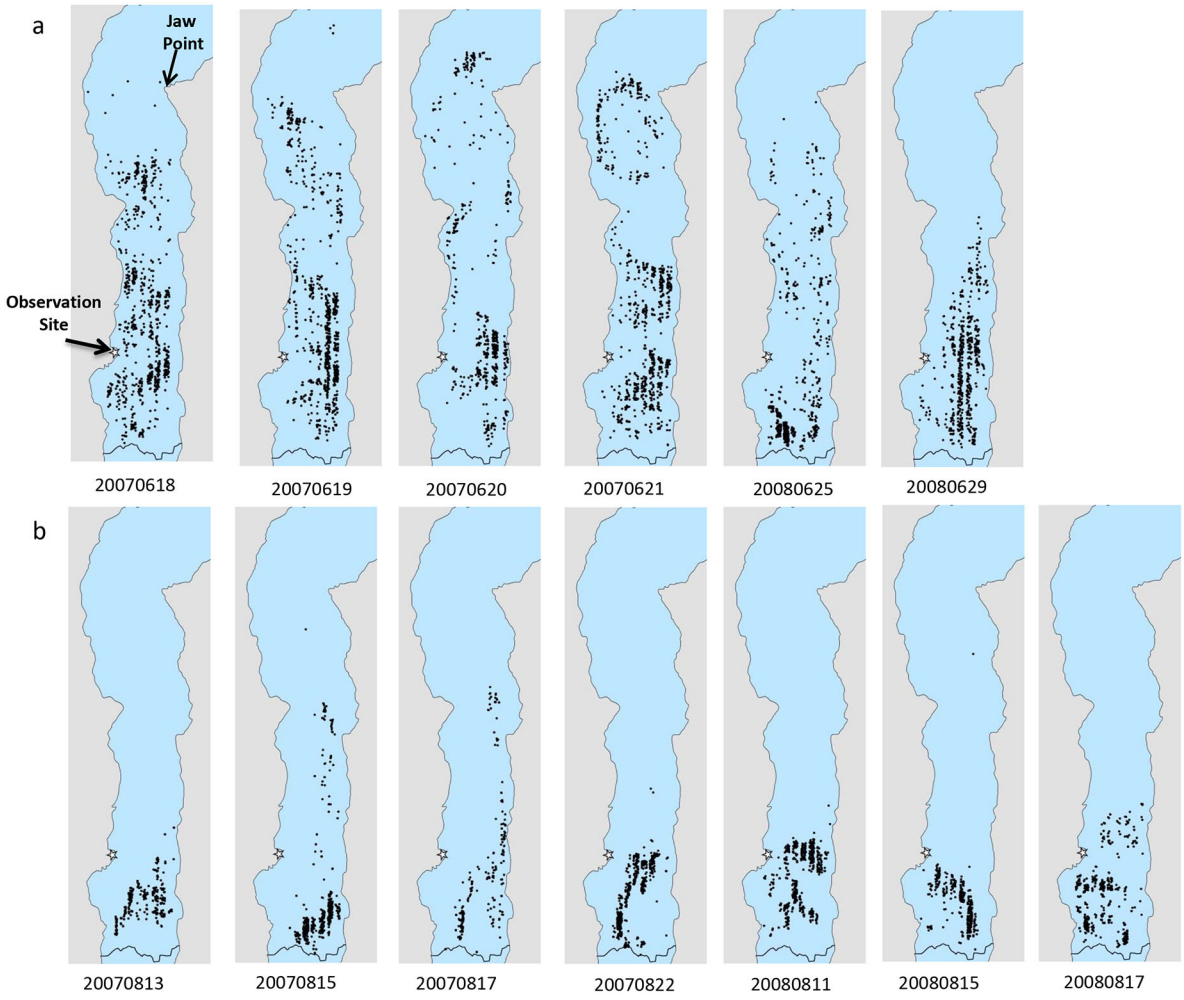

Fig. 3. Distribution of harbor seals in Johns Hopkins Inlet, Glacier Bay National Park, from aerial photographic surveys during the pupping season in June (a) and the molting season in August (b) during 2007 and 2008. Filled black circles represent seals along transects. White star indicates location of shore-based observation site.

In other words, we borrow strength in estimating the autocorrelation parameters by assuming each year is another realization of the same temporally autocorrelated process for survey period j.

We assumed $Y_{j,g,\ell}(i,t_j,r) \sim \mathcal{L}\left(\mu_{j,g,\ell}(i,t_j),\nu\right)$ for shore-based counts and $Y_{j,a,\ell}(i,t_j,r) \sim \mathcal{L}\left(\mu_{j,a,\ell}(i,t_j),\nu + V_{j,\ell}(i,t_j)\right)$ for aerial surveys, where $V_{j,\ell}(i,t_j)$ is the estimated coefficient of variation from aerial surveys for pups ($\ell = u$) or nonpups ($\ell = n$) on the tth day of the jth season in the ith year using the method of Ver Hoef and Jansen (2015). All models were fit assuming a Bayesian hierarchical model structure (Cressie et al. 2009) using Markov Chain Monte Carlo (MCMC) methods (Gelfand and Smith, 1990). Details are provided in the Supplemental Material. We obtained 1000 samples from the posterior distributions from all parameters and quantities of interest for further adjustment to estimated abundance and trend, which we describe next.

Haul-out models

A haul-out model was developed, using the previously described data collected from satellite-linked transmitters that were attached to harbor seals, to estimate the proportion of time that seals spend in the water. This is necessary to adjust counts of hauled out seals to estimate abundance.

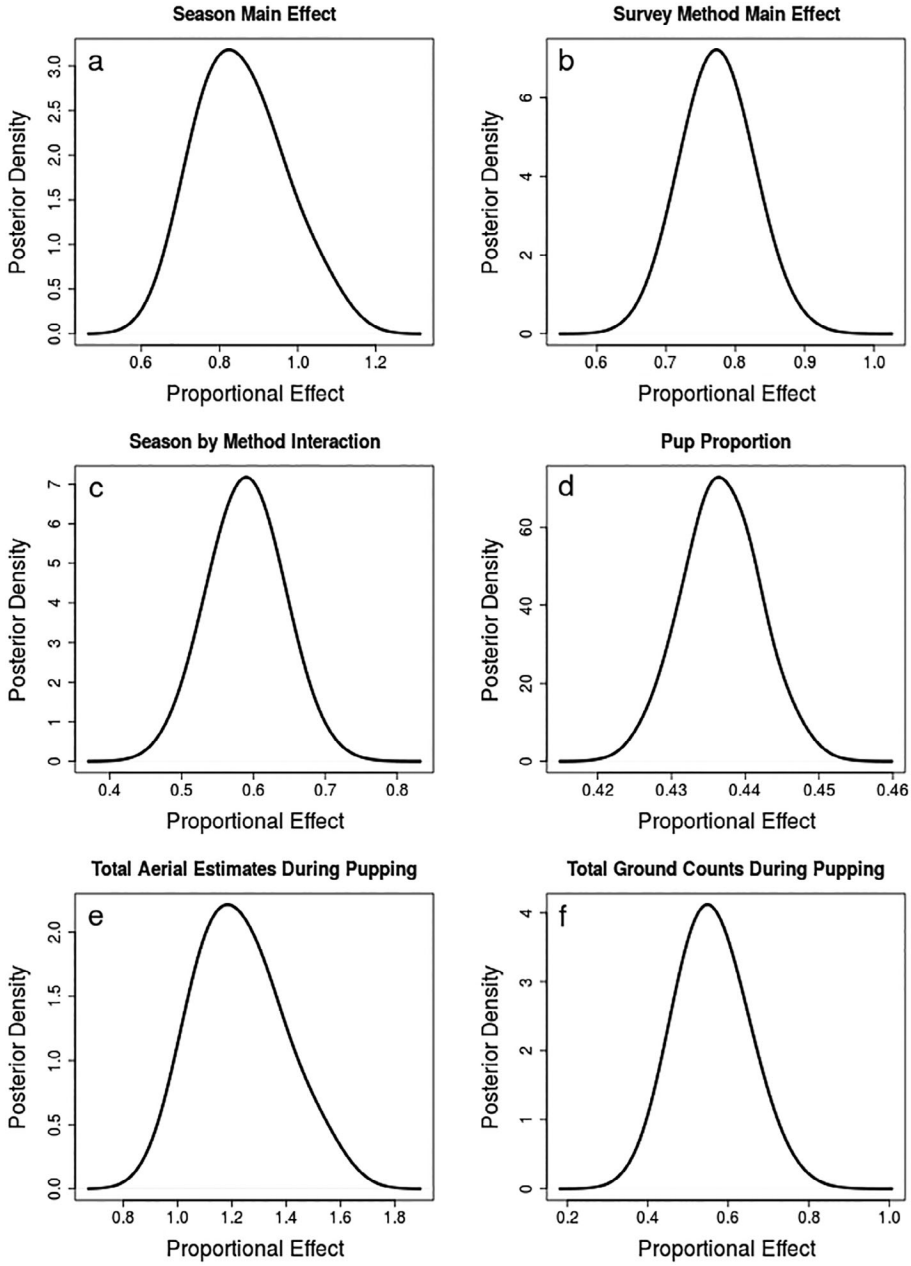

Fig. 4. Posterior densities of proportional effects computed from linear model components in Eq. 3. All effects are proportional to aerial counts during molting.

Let $H_{i,q}$ be a random variable for haul-out for animal i for the qth hour of the summer, where recall that $h_{i,q} \in \mathcal{H} \equiv \{0, 0.025, 0.1, 0.2, 0.3, 0.4, 0.5, 0.6, 0.7, 0.8, 0.9, 0.975, 1\}$. We built a model for the molting season only (any hour on, or after, the 16th of July, through 30 September), as all counts were corrected to this season. We modeled $H_{i,q}$ using beta regression (Ferrari and Cribari-Neto, 2004, Cribari-Neto and Zeileis, 2010),

$$H_{i,q} \sim \text{Beta}\left(\theta_{i,q}, \gamma\right).$$

Here, the beta density function is parameterized as,

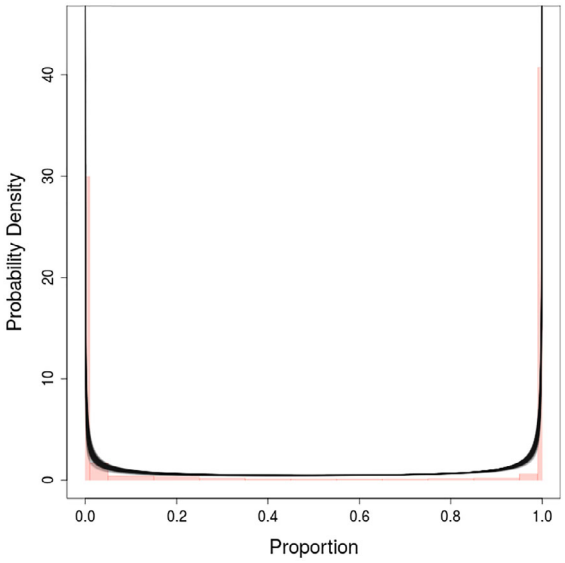

Fig. 5. Raw histogram (red bars) and 1000 MCMC samples (semitransparent black lines) of the fitted beta distribution (standardized to 15 August) for haul-out data.

$$f(h;\theta,\gamma)=\frac{\Gamma(\theta)}{\Gamma(\theta\gamma)\Gamma((1-\theta)\gamma)}h^{\theta\gamma-1}(1-h)^{(1-\theta)\gamma-1} \quad (6)$$

where $0<h<1$, $0<\theta<1$, and $\gamma>0$. Notice that the range for h is strictly greater than 0 and less than 1, yet $\mathcal{H}$ contains both 0 and 1. In this case, it is possible to use zero-one-inflated beta regression (Ospina and Ferrari, 2010, 2012), but that requires modeling the zeros and ones as separate regressions, and in general assumes that the processes that generate them are different than the process generating the values between 0 and 1. An alternative is to transform the zeros to small values that are close to 0, and the ones to values that are just less than 1. We adopted the suggestion by Smithson and Verkuilen (2006) (also recommended by Cribari-Neto and Zeileis, 2010) such that.

$$h^*=\frac{h(n-1)+0.5}{n}$$

where n is the sample size; i.e., we replaced all $h_{i,q}=0$ or $h_{i,q}=1$ with h^* as given above.

We modeled haul out with a seasonal trend, random effects for animals, and temporal autocorrelation for repeated measurements on an animal. Note that for Eq. 6, $E(H)=\theta$ and $\text{var}(H)=\theta(1-\theta)/(1+\gamma)$. Then, for beta regression, we let.

$$\text{logit}(\theta_{i,t})=\beta_0+\beta_1 t+\beta_2 t^2+T_i(q)+A_i \quad (7)$$

where β_0 is an overall mean effect, β_1 and β_2 are regression effects that allow a quadratic trend over day-of-year t, $T_i(q)$ is a temporally autocorrelated random effect, and A_i is a random effect for the ith animal. For temporal autocorrelation within the ith animal, we used an AR1 model,

$$T_i(q)=\alpha T_i(q-1)+\zeta\varepsilon_{i,q} \quad (8)$$

where $0\le\alpha\le1$ and $\{\varepsilon_{i,q}\}$ are standard normal random variables that are independent for all i,q, $T_i(1)$ is 0, and all $T_i(q)$ are independent across animals. Note that the autocorrelation parameter, α, and variance parameter, ζ, are shared among animals, but we assume animals are independent of each other. We did not include time of day as a fixed effect because, when tested, there was little effect, and it was not an effect in the count model (there was little variation in time of day for counts). Instead, we accounted for time of day as an autocorrelated random effect. All models were fit assuming a Bayesian hierarchical model using Markov Chain Monte Carlo (MCMC) methods. Details are provided in the Appendix S1. We obtained 1000 samples from the posterior distributions from all parameters and quantities of interest.

Abundance and trend

For all parameters and variables sampled from the posterior distribution, we use a superscript in brackets, [g], to denote the gth retained MCMC sample, so $g=1,\ldots,1000$. For example, $\eta^{[g]}$ is the gth MCMC sample of η. For a single MCMC sample, a standardized aerial survey count estimate, for the 15th day of August during the molting period, in the ith year, was estimated as,

$$C_i^{[g]}=\eta^{[g]}+N_i^{[g]}+\overline{Z}_m(i,15) \quad (9)$$

where $\overline{Z}_m(i,15)$ is the average, over all MCMC samples of the random effect $Z_m(i,15)$ for the ith year for the 15th of August. We averaged over the MCMC samples because we were not interested in the uncertainty for the daily effect; rather just the year. However, because $Z_m(i,t_j)$ is autocorrelated, the average on any particular day may well be away from zero (especially because daily trends are captured by $Z_m(i,t_j)$. Then, the estimated count for the ith year was the mean of $C_i^{[g]}$ over the g MCMC samples, and the credible

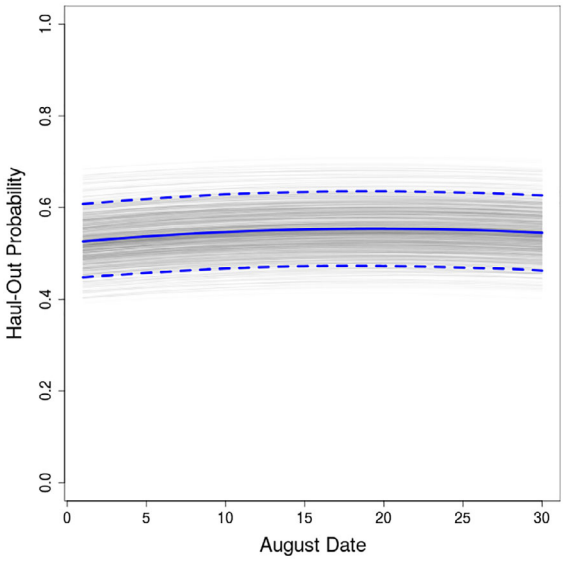

Fig. 6. 1000 MCMC samples, shown as semitransparent gray lines, of the effect of date on haul-out probability of harbor seals monitored by satellite telemetry. The mean haul-out probability, as a function of data, is given by the solid blue line, and the 95% credible intervals are given by the dashed blue lines.

intervals were obtained from the quantiles of $\left\{C_i^{[g]}; g = 1, \ldots, 1000\right\}$.

The count estimates are uncorrected for the proportion of seals in the water. For the haulout model (7), again let $[g]$ denote the gth retained MCMC sample; for example, $\beta_0^{[g]}$ is the gth MCMC sample of β_0. Then, for a single MCMC sample, a standardized abundance estimate, for the 15th day of August during the molting period, in the ith year, was estimated as,

$$\mathcal{A}_i^{[g]} = \frac{C_i^{[g]}\left(1 - \exp\left(\beta_0^{[g]}\right)\right)}{\exp\left(\beta_0^{[g]}\right)} \quad (10)$$

Note that we are dividing the expected counts by the expected probability of haulout to obtain abundance estimates for arbitrarily matched MCMC samples from the posterior distributions from the count models and the haulout models. Then, the estimated abundance for the ith year was the mean of $\mathcal{A}_i^{[g]}$ over the g MCMC samples,

$$\hat{\mathcal{A}}_i = \frac{\sum_{g=1}^{1000} \mathcal{A}_i^{[g]}}{1000} \quad (11)$$

and the credible intervals were obtained from the quantiles of $\left\{\mathcal{A}_i^{[g]}; g = 1, \ldots, 1000\right\}$.

For trend, let $\mathcal{T}_{i,\ell}^{[g]} = \{\mathcal{A}_i, \ldots, \mathcal{A}_{i+\ell-1}\}$, and let $\Delta_{i,\ell}^{[g]}$ be the slope coefficient of the linear regression of $\mathcal{T}_{i,\ell}^{[g]}$ on $\{1, 2, \ldots, \ell\}$. Then, the estimated trend of the ℓ years, beginning in the ith year, was the mean of $\Delta_{i,\ell}^{[g]}$ over the g MCMC samples,

$$\hat{\Delta}_{i,\ell} = \frac{\sum_{g=1}^{1000} \Delta_{i,\ell}^{[g]}}{1000} \quad (12)$$

and credible intervals were obtained from the quantiles of $\left\{\Delta_{i,\ell}^{[g]}; g = 1, \ldots, 1000\right\}$. The R package for the code can be found here: https://github.com/jayverhoef/JHop

Results

Shore-based counts, aerial photographic surveys, and calibration

During 2007 and 2008, counts of seals by shore-based observers during June, for both pups and nonpups, were substantially lower than estimates from aerial photographic surveys on the same day (Fig. 2a, b). During June, seals were distributed extensively throughout the fjord from near the terminus of the Johns Hopkins Glacier, and on a few days beyond Jaw Point, approximately 11 km away from the shore-based observation site (Fig. 3a). In contrast, during the molting season in August, counts of nonpups by shore-based observers were more similar, but still less than the number estimated from aerial photographic surveys (Fig. 2c). In August, seals were clustered closer to the terminus of the glacier, typically ranging no more than 3.5–4.0 km away (Fig. 3b).

Fig. 4a–f shows the posterior distributions, using kernel density estimate of 1000 MCMC samples, of calibration and standardization effects in Eq. 3, and corroborates the results from the raw data presented in Fig. 2. The zero states of ξ_j, τ_k, $\xi\tau_{j,k}$, and $\xi\pi_{j,\ell}$ occur for aerial surveys of nonpups during the molting season. Therefore, each of the aforementioned effects are proportional to aerial surveys of nonpups during the molting season when the linear model Eq. 3 is exponentiated. Counts of seals during the molting season were about 85% of counts during the pupping season (Fig. 4a). Shore-based counts

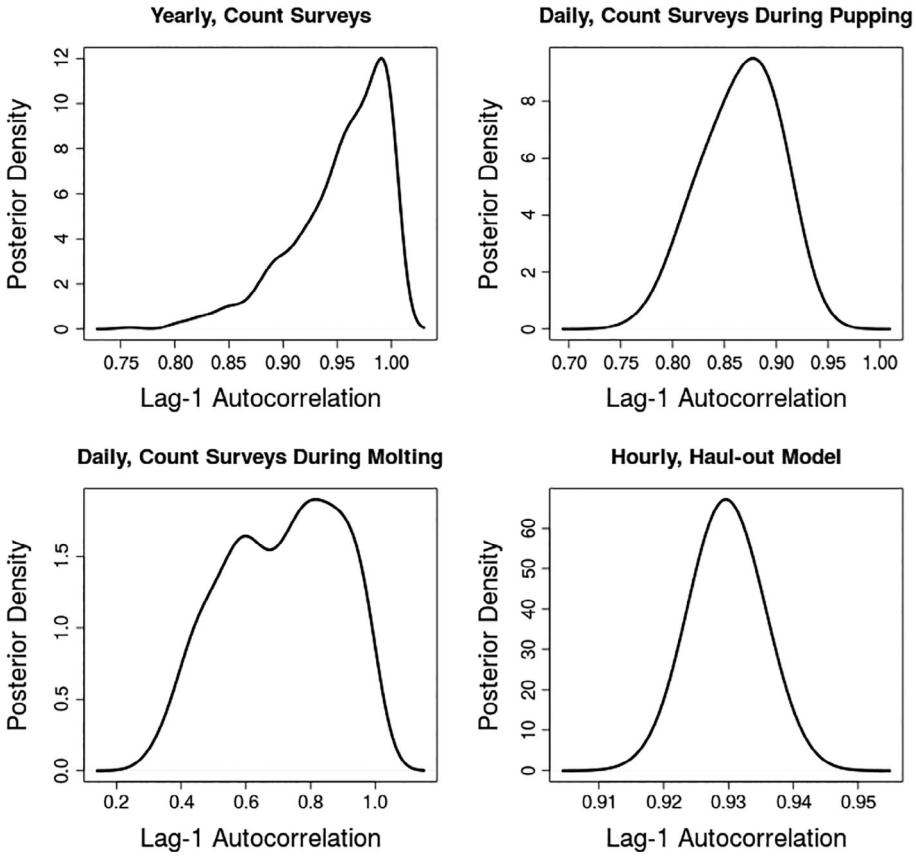

Fig. 7. Posterior densities for all autocorrelation parameters. The yearly autocorrelation for count surveys is ϕ in Eq. 4. The daily autocorrelation for count surveys during pupping is ω_p in Eq. 4, and during molting is ω_m. The hourly autocorrelation parameter is α in Eq. 8.

were slightly less than 80% of aerial survey estimates (Fig. 4b); however, there was a significant interaction between survey method and season. Shore-based counts during the pupping season were approximately 60% lower than what would be predicted by main effects alone (Fig. 4c). The proportion of pups, which is an interaction term without main effect for season, and thus operated only during pupping season, had a posterior distribution with a mode centered at about 44% of aerial survey estimates of nonpups during the molting season (Fig. 4d).

To ascertain the overall effect of season and method on count estimates, the posterior distribution of $\exp(\xi_p) + \exp(\xi_p + \xi\pi_{p,u})$, which is the aerial survey estimate of nonpups plus pups for the pupping period, has a mode at about 20% higher than the molting season (Fig. 4e). Shore-based counts are about 60% of aerial survey estimates during pupping season (Fig. 4f), computed as the posterior distribution of $\exp(\xi_p + \tau_g + \xi\tau_{p,g}) + \exp(\xi_p + \tau_g + \xi\tau_{p,g} + \xi\pi_{p,u})$. The comparison of shore-based counts to aerial survey estimates during molting season is given directly by the main effect in Fig. 4b.

Estimating proportion of seals hauled out to adjust counts

Using data collected from satellite-linked transmitters that were attached to harbor seals, beta regression was used to model haulout. The raw proportion of seals hauled out is given in Fig. 5, and the 1000 posterior fits of the beta distribution (Eq. 6), using only $\beta_0 = \theta$ from Eq. 7, are given as semitransparent gray lines. Fig. 5 shows that seals tended to be either completely hauled out, or at sea, for whole hours. The fitted beta distribution reflected that pattern. The effect of date on haulout

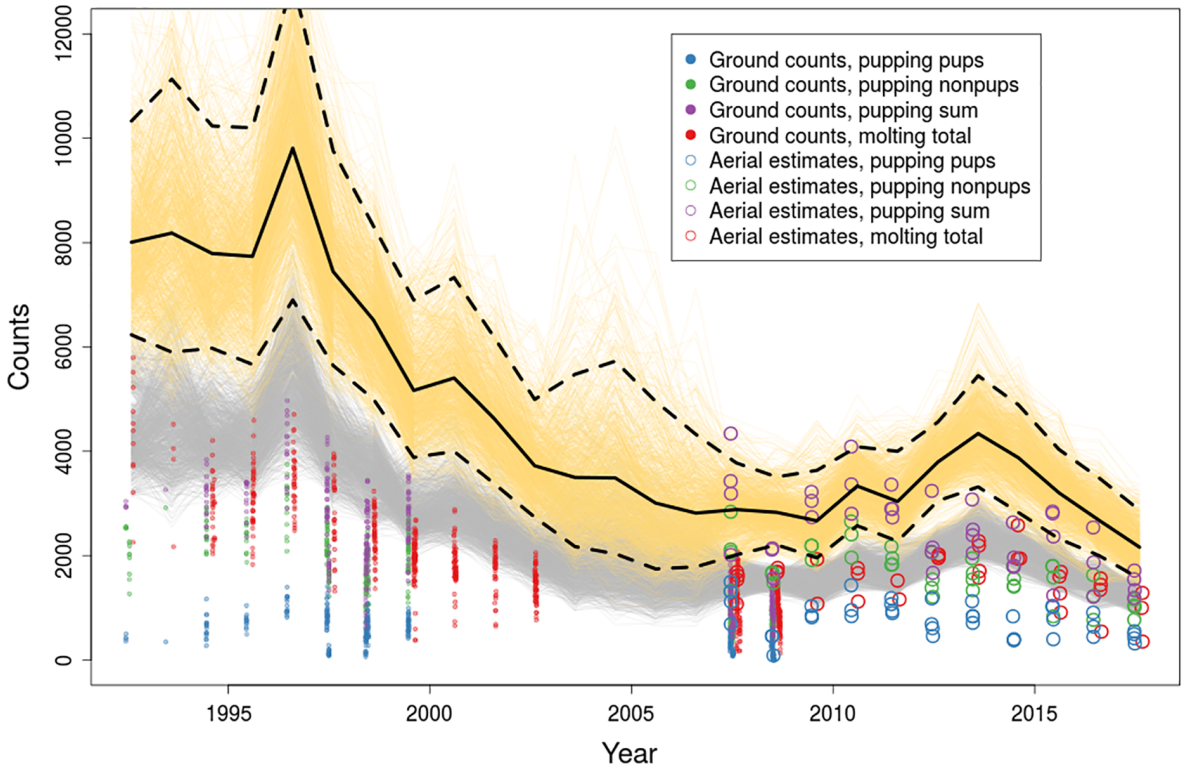

Fig. 8. Abundance and trends of harbor seals in Johns Hopkins Inlet from 1992 to 2017. Raw shore-based counts and aerial survey estimates are shown as circles. 1000 MCMC samples of the fitted model, adjusted to 15 August for aerial surveys, are shown as semitransparent gray lines. 1000 MCMC samples of abundance, including an additional adjustment for haul out, are shown as semitransparent orange lines. The mean of the MCMC abundance estimates is the thick, solid black line, and the 90% credible intervals are given by the thick, dashed black lines.

is shown in Fig. 6, where the proportion of time that seals are hauled out is between 50 and 55%, and there is very little change during August. The posterior distributions of all AR1 autocorrelation parameters are shown in Fig. 7, showing substantial temporal autocorrelation for all submodels.

Abundance and trends from adjusted counts from 1992 to 2017

After calibrating the shore-based counts to the aerial surveys and estimating the proportion of seals hauled out to adjust counts, data were combined across years to generate standardized estimates of abundance and trend from 1992 to 2017. The estimated abundance of seals (Eq. 11), fit to the raw counts at standardized covariates (15 August, gray lines) and then adjusted for the proportion of seals in the water (orange lines), along with raw counts and aerial survey estimates, is given in Fig. 8. Estimated abundance was highest from 1992 through 1997, with a high of 9810 seals (95% CI: 6478–13699) in 1996. Over the most recent 10-yr period (2008–2017), the estimated abundance of seals ranged from 4341 seals (95% CI: 3101–5877) in 2013 to 2163 seals (95% CI: 1499–3010) in 2017 (Table 3).

Over the 26-yr period, the standardized estimated trend (Eq. 12) for seals in Johns Hopkins Inlet is negative (Table 4). Trends computed for 10-yr time intervals, incremented yearly, show that the steep and significant declines ended around 2011 (Table 5), with leveling off and possibly some subsequent recovery up through 2013 (Fig. 8). The most recent shorter-term (2013–2017) trends, however, are steeply negative again, rivaling the steepest declines (Table 4).

Table 3. Estimated abundances of harbor seals in Johns Hopkins Inlet from 1992 to 2017.

Year	Low95	Low90	Mean	Upp90	Upp95
1992	5981	6231	8009	10,330	10,706
1993	5628	5899	8183	11,131	11,783
1994	5752	5975	7792	10,235	10,894
1995	5416	5665	7737	10,200	10,716
1996	6478	6898	9810	13,027	13,699
1997	5428	5646	7448	9764	10,168
1998	4794	4999	6518	8318	8769
1999	3698	3882	5167	6899	7272
2000	3748	3999	5404	7331	7732
2001	3182	3378	4623	6180	6553
2002	2603	2737	3724	4995	5242
2003	2017	2174	3499	5475	6227
2004	1906	2036	3489	5727	6391
2005	1616	1747	3008	4955	5409
2006	1616	1787	2816	4323	4638
2007	1874	2014	2884	3778	3963
2008	2130	2209	2831	3509	3641
2009	1859	1959	2669	3635	3875
2010	2466	2574	3335	4087	4219
2011	2163	2278	3039	4001	4250
2012	2759	3050	3796	4561	4681
2013	3101	3318	4341	5448	5877
2014	2702	2827	3875	4889	5095
2015	2194	2325	3207	4038	4173
2016	1649	2001	2677	3488	3587
2017	1499	1563	2163	2872	3010

Notes: Low95 and Low90 are the lower 95% and 90% credible intervals, respectively, and Upp95 and Upp90 are the upper 95% and 90% credible intervals, respectively. The mean of the posterior distribution is used as the abundance estimate.

Table 4. Estimated trends of harbor seals in Johns Hopkins Inlet to 2017, starting from 2013, and going progressively backwards year by year to the starting year in 1992.

Year	Low95	Low90	Mean	Upp90	Upp95
2013–2017	−914	−828	−555	−301	−270
2012–2017	−618	−579	−395	−217	−178
2011–2017	−359	−338	−214	−74	−52
2010–2017	−270	−255	−146	−25	−14
2009–2017	−154	−144	−60	61	69
2008–2017	−88	−81	−21	64	72
2007–2017	−64	−57	−2	57	65
2006–2017	−77	−60	12	72	80
2005–2017	−105	−85	14	84	95
2004–2017	−153	−124	0	87	94
2003–2017	−172	−135	−8	77	86
2002–2017	−154	−126	−19	54	62
2001–2017	−160	−133	−44	22	30
2000–2017	−176	−157	−74	−10	−2
1999–2017	−194	−173	−90	−32	−23
1998–2017	−206	−188	−121	−70	−61
1997–2017	−228	−215	−153	−101	−91
1996–2017	−293	−278	−204	−141	−129
1995–2017	−312	−294	−218	−153	−139
1994–2017	−328	−305	−227	−167	−153
1993–2017	−331	−315	−236	−176	−162
1992–2017	−333	−316	−239	−181	−173

Notes: Low95 and Low90 are the lower 95% and 90% credible intervals, respectively, and Upp95 and Upp90 are the upper 95% and 90% credible intervals, respectively. The mean of the posterior distribution is used as the trend estimate.

Discussion

Simultaneous shore-based and aerial photographic surveys of seals in 2007 and 2008 were used to generate an analytical calibration between the two methods and allowed standardized abundance and trend estimates over the 26-yr period from 1992 to 2017. Shore-based counts of seals were less than estimates from aerial photographic surveys, particularly during the pupping season in June (Fig. 2a). The higher estimates of seals from aerial photographic surveys were likely related to the fact that aerial surveys spanned the length and width of the fjord, provided a vertical rather oblique perspective, and eliminated bias associated with field observers counting at variable distances and low angles relative to seals.

Previous studies also found that counts of seals from aerial photographic surveys were typically higher than counts by shore-based observers and that both methods encountered challenges associated with double-counting and missing seals, particularly due to movement of ice that resulted in seals drifting between survey zones (Mathews et al. 1997, Bengtson et al. 2007). Many of the limitations of counting seals from a shore-based site were addressed by aerial photographic surveys. Seals that were photographed along a transect, regardless of the location, had the same probability of being sampled (Ver Hoef and Jansen 2015). Aerial photographic surveys can be completed in one hour, and thus, the likelihood of seals moving into or leaving the study area is less than for shore-based counts, which typically take longer to complete. In addition, the permanent photographic record generated from aerial surveys allows for re-examination of images for retrospective studies (Buckland et al. 2012), development of automated methods for counting of seals from the imagery (Conn et al. 2014, Seymour et al. 2017), and can be

Table 5. Estimated trends of harbor seals in Johns Hopkins Inlet over 10-yr periods, incremented yearly beginning in 1992, to present day.

Year	Low95	Low90	Mean	Upp90	Upp95
1992–2001	−704	−657	−419	−208	−166
1993–2002	−838	−791	−538	−308	−262
1994–2003	−929	−870	−607	−385	−338
1995–2004	−1005	−940	−645	−416	−377
1996–2005	−1029	−962	−661	−427	−382
1997–2006	−791	−742	−492	−270	−205
1998–2007	−604	−561	−393	−232	−208
1999–2008	−471	−442	−302	−188	−166
2000–2009	−451	−419	−266	−153	−134
2001–2010	−356	−311	−147	−21	−2
2002−2011	−312	−275	−72	78	97
2003–2012	−297	−237	4	180	204
2004–2013	−172	−126	94	261	289
2005–2014	−31	4	147	269	297
2006–2015	2	27	128	221	240
2007–2016	−21	−6	64	131	142
2008–2017	−88	−81	−21	64	72

Notes: Low95 and Low90 are the lower 95% and 90% credible intervals, respectively, and Upp95 and Upp90 are the upper 95% and 90% credible intervals, respectively. The mean of the posterior distribution is used as the trend estimate.

extended to unmanned aerial systems (Sweeney et al. 2015, Moreland et al. 2015).

Counts of seals during the molting season were about 85% of counts during the pupping season as indicated by a significant interaction between survey method and season. However, this pattern is in contrast to previous studies that documented higher numbers of seals during the molting period from 1992 to 2002 (Mathews and Pendleton, 2006). A key environmental variable that likely influences the distribution and abundance of seals between the pupping and molting seasons is floating glacier ice and icebergs, which seals use as a resting substrate. Ice availability changes seasonally in Johns Hopkins Inlet and is typically greatest in spring and early summer, when frontal ablation of the glacier tends to be highest (McNabb et al. 2015). During 2007 and 2008, the amount of ice in survey photographs was consistently greater during the pupping season than during the molting season (*unpublished data*). In addition, during the molting season ice tends to concentrate primarily near the glacier, which suggests that the distribution of ice is a factor that may influence the seasonal distribution and abundance of seals. In Disenchantment Bay, Alaska, Jansen et al. (2015) also found that ice cover was a factor that influenced the distribution of harbor seals.

Although the majority of tidewater glaciers are thinning and retreating (Arendt et al. 2002, Larsen et al. 2007), the Johns Hopkins Glacier is one of the few advancing tidewater glaciers in Alaska (McNabb and Hock, 2014). Yet, how iceberg availability changes with the advance and retreat of tidewater glaciers is not well understood. If tidewater glaciers continue to thin and retreat, the amount of ice habitat that is available for harbor seals is expected to decrease and seals may spend more time in the water, use terrestrial sites, or move to other areas (Calambokidis et al. 1987, Womble et al. 2010). As an example, in the early 1990s the Muir Glacier in the East Arm of Glacier Bay, retreated rapidly, and eventually grounded. Prior to the grounding of the Muir Glacier, over 1,100 harbor seals were counted on icebergs at the terminus of Muir Glacier in the 1970s and 1980s (Streveler, 1979, Calambokidis et al. 1987), and by 1993, none were observed (Mathews and Pendleton, 2006). Thus, understanding the mechanistic linkages between glacier advance and retreat, factors that influence calving dynamics of glaciers, and iceberg production (Amundson, 2016, Amundson and Carroll, 2017) will be essential for predicting the response of seals to changes in ice availability in tidewater glacier fjords.

In addition, life-history events may also influence the abundance of seals and contribute to higher counts of seals during the pupping, compared to the molting, season. Adult female seals with a dependent pup may spend more time hauled out on ice to give birth and nurse their young. Once pups are weaned approximately 3–5 weeks after birth, adult females are no longer as restricted to the ice habitat and may travel outside of Johns Hopkins Inlet to forage where prey tend to be more abundant and shallow (Womble and Gende, 2013, Womble et al. 2014). If adult females spend more time foraging and less time hauled out after pups are weaned, this could result in a decrease in abundance of seals after the pupping season.

From count data alone, it is not possible to estimate how many seals are at sea and not available to be counted during surveys, which is essential for estimating total abundance (Boveng et al. 2003, Lonergan et al. 2013). Using data collected

from satellite-linked transmitters that were attached to harbor seals, the haul-out model revealed that the proportion of time that seals hauled out was relatively consistent during the molting period in August (0.50 to 0.55) (Fig. 6). This result was used to adjust counts to estimate total abundance over the 26-yr period. By adjusting the counts, the estimated total abundance across all years was substantially greater across the entire study period compared to previous estimates, which did not account for the proportion of seals at sea and represented the minimum number of seals in the fjord (Mathews and Pendleton, 2006, Womble et al. 2010). Although haul-out behavior of seals may vary depending upon seal age and sex, location, habitat, and season (Huber et al. 2001, Simpkins et al. 2003, Harvey and Goley, 2011), estimating the total abundance of seals is critical for understanding the status of populations, informing management decisions that assess actual and potential impacts on populations, as well as for detecting recovery of populations (Taylor et al. 2000, 2007).

By generating a calibration technique between the two methods and adjusting the counts to estimate abundance, we were able to ascertain important fluctuations in trend that would not have been apparent had we (1) continued shore-based counts or (2) transitioned to aerial photographic surveys without being able to use the data collected during shore-based counts. Over the 26-yr period from 1992 to 2017, the standardized estimated trend for harbor seals in Johns Hopkins Inlet was negative; however, there has generally been an increasing trend over the 13-yr period from 2005 to 2017. Yet, in the most recent years (2016–2017), the estimated abundance of seals has decreased (Table 3).

It is currently unknown what factors may contribute to changing population trajectories for harbor seals in Johns Hopkins Inlet. Precipitous declines in harbor seals also occurred in other regions of Alaska (Pitcher, 1990, Frost et al. 1999); however, recent evidence suggests that the declines at some sites have abated (Jemison et al. 2006, Hoover-Miller and Armato, 2017). Collectively, these oscillating patterns in population trajectories of seals suggest that larger-scale factors may have played a role. Large-scale physical and biological changes occurred in the Northeast Pacific in the 1970s with a regime shift in 1976–1977 (Miller et al. 1994, Trenberth and Hurrell, 1994). Ocean temperatures shifted from cooler to warmer, and there was a subsequent reorganization in community structure and species composition in the western and central Gulf of Alaska (Anderson and Piatt, 1999). The pattern of warmer ocean temperatures persisted for over three decades and was associated with declines in several upper-trophic level species. In 2008, there was a shift from warmer to cooler ocean temperatures with some indications that there may have been a reversal of the 1976–1977 regime shift (Hatch, 2013). Our long-term analysis reveals evidence for a similar pattern, where numbers of harbor seals declined from 1997 to 2008, stabilized, and then increased through 2013 (Fig. 8).

In more recent years, anomalously warm waters persisted in the eastern Gulf of Alaska from 2014 to 2016 due to a combination of a large warm water mass and a strong El Niño (Bond et al. 2015). Changes in lower trophic levels (Batten et al. 2018), a decreased abundance of Pacific herring in the eastern Gulf of Alaska (Strasburger et al. 2018), and lower abundance estimates for harbor seals in 2016 and 2017 coincide with increases in water temperature, a factor that influences the organization of marine communities and biological responses in the North Pacific Ocean (Francis et al. 1998).

Our case study with harbor seals in Johns Hopkins Inlet in Glacier Bay provides an example of the value of development of a calibration between two monitoring methods to improve the sensitivity of long-term monitoring to detect changes in abundance for a species of conservation concern and consistency with monitoring methods that are used for seals in tidewater glacier ice sites throughout Alaska. Most importantly, the calibration of historical and current data sets allowed us to assess finer-scale and long-term fluctuations in abundance that would not have otherwise been feasible. Long-term ecological monitoring that provides robust abundance estimates and trends is essential for linking biological patterns to environmental variability and informing management decisions that may help to conserve these species. Understanding mechanistic linkages between bottom-up and top-down processes, vital rates, and population trajectories is critical for interpreting patterns in abundance; however, elucidating these relationships can be challenging, particularly given the complexity of the marine environment.

Establishing rigorous long-term monitoring programs for species of conservation concern provides essential baseline and trend data that are vital for understanding how populations are responding to rapidly changing environments.

Acknowledgments

Numerous individuals provided essential field, data processing, logistical, and administrative support including John Jansen, Josh London, Linnea Pearson, Louise Taylor-Thomas, Melissa Senac, Evelina Augustton, Colleen Young, Natalie Bool, Trevor Ose, Monika Becker, Norma Vasquez, Carol Coyle, Lara Dzinich, Janene Driscoll, Shawn Dahle, Lisa Etherington, Lewis Sharman, Margaret Hazen, and staff at the Glacier Bay National Park and Preserve Visitor Information Station. Avery Gast, Dennis Lozier, Jacques Norvell, and Chuck Schroth provided aerial survey expertise. Justin Smith provided vessel support on the R/V *Capelin*. We appreciate constructive comments provided on earlier drafts by M. Bower and anonymous reviewers. Funding and logistical support was provided by Glacier Bay National Park and Preserve, Glacier Bay National Park Marine Management Fund, NOAA Fisheries, Alaska Fisheries Science Center Marine Mammal Laboratory, and Ocean Alaska Science and Learning Center.

Literature Cited

Amundson, J. M. 2016. A mass-flux perspective of the tidewater glacier cycle. Journal of Glaciology 62:82–93.

Amundson, J. M., and D. Carroll. 2017. Effect of topography on subglacial discharge and submarine melting during tidewater glacier retreat. Journal of Geophysical Research: Earth Surface 123:66–79.

Anderson, P. J., and J. F. Piatt. 1999. Community reorganization in the Gulf of Alaska following ocean climate regime shift. Marine Ecology Progress Series 189:117–123.

Arendt, A. A., K. A. Echelmeyer, W. D. Harrison, C. S. Lingle, and V. B. Valentine. 2002. Rapid wastage of Alaska glaciers and their contribution to rising sea level. Science 297:382–386.

Baker, J. D., A. L. Harting, T. C. Johanos, and C. L. Littnan. 2016. Estimating Hawaiian monk seal range-wide abundance and associated uncertainty. Endangered Species Research 31:317–324.

Batten, S. D., D. E. Raitsos, S. Danielson, R. Hopcroft, K. Coyle, and A. McQuatters-Gollop. 2018. Interannual variability in lower trophic levels on the Alaskan shelf. Deep Sea Research Part II: Topical Studies in Oceanography 147:58–68.

Beauchamp, J. J., and J. S. Olson. 1973. Corrections for bias in regression estimates after logarithmic transformation. Ecology 54:1403–1407.

Bengtson, J. L., A. V. Phillips, E. A. Mathews, and M. A. Simpkins. 2007. Comparison of survey methods for estimating abundance of harbor seals (*Phoca vitulina*) in glacial fjords. Fishery Bulletin 105:348–356.

Blundell, G. M., J. N. Womble, G. W. Pendleton, S. A. Karpovich, S. M. Gende, and J. K. Herreman. 2011. Use of glacial and terrestrial habitats by harbor seals in Glacier Bay, Alaska: Costs and benefits. Marine Ecology Progress Series 429:277–290.

Bond, N. A., M. F. Cronin, H. Freeland, and N. Mantua. 2015. Causes and impacts of the 2014 warm anomaly in the NE Pacific. Geophysical Research Letters 42:3414–3420.

Boveng, P. L., J. L. Bengtson, D. E. Withrow, J. C. Cesarone, M. A. Simpkins, K. J. Frost, and J. J. Burns. 2003. The abundance of harbor seals in the Gulf of Alaska. Marine Mammal Science 19:111–127.

Boveng, P. L., J. M. Ver Hoef, D. E. Withrow, and J. M. London. 2018. A Bayesian analysis of abundance, trend, and population viability for harbor seals in Iliamna Lake, Alaska. Risk Analysis 38:1988–2009.

Buckland, S. T., M. L. Burt, E. A. Rexstad, M. Mellor, A. E. Williams, and R. Woodward. 2012. Aerial surveys of seabirds: The advent of digital methods. Journal of Applied Ecology 49:960–967.

Calambokidis, J., B. L. Taylor, S. D. Carter, G. H. Steiger, P. K. Dawson, and L. D. Antrim. 1987. Distribution and haul-out behavior of harbor seals in Glacier Bay, Alaska. Canadian Journal of Zoology 65:1391–1396.

Conn, P. B., J. M. Ver Hoef, B. T. McClintock, E. E. Moreland, J. M. London, M. F. Cameron, S. P. Dahle, and P. L. Boveng. 2014. Estimating multispecies abundance using automated detection systems: ice-associated seals in the Bering Sea. Methods in Ecology and Evolution 5:1280–1293.

Cressie, N., K. A. Calder, J. S. Clark, J. M. Ver Hoef, and C. K. Wikle. 2009. Accounting for uncertainty in ecological analysis: The strengths and limitations of hierarchical statistical modeling. Ecological Applications 19:553–570.

Cribari-Neto, F., and A. Zeileis. 2010. Beta regression in R. Journal of Statistical Software 34:1–24.

Crowell, A. L. 2016. Ice, seals, and guns: Late 19th-century Alaska native commercial sealing in Southeast Alaska. Arctic Anthropology 53:11–32.

Ferrari, S., and F. Cribari-Neto. 2004. Beta regression for modelling rates and proportions. Journal of Applied Statistics 31:799–815.

Francis, R. C., S. R. Hare, A. B. Hollowed, and W. S. Wooster. 1998. Effects of interdecadal climate

variability on the ocean ecosystems of the NE Pacific. Fisheries Oceanography 7:1–21.

Frost, K. J., L. F. Lowry, and J. M. Ver Hoef. 1999. Monitoring the trend of harbor seals in Prince William Sound, Alaska, after the Exxon Valdez oil spill. Marine Mammal Science 15(2):494–506.

Gelfand, A. E., and A. F. M. Smith. 1990. Sampling-based approaches to calculating marginal densities. Journal of the American Statistical Association 85:398–409.

Goodman, D. 2004. Methods for joint inference from multiple data sources for improved estimates of population size and survival rates. Marine Mammal Science 20:401–423.

Harvey, J. T., and D. Goley. 2011. Determining a correction factor for aerial surveys of harbor seals in California. Marine Mammal Science 27:719–735.

Hatch, S. A. 2013. Kittiwake diets and chick production signal a 2008 regime shift in the Northeast Pacific. Marine Ecology Progress Series 477:271–284.

Hoover-Miller, A., and P. Armato. 2017. Harbor seal use of glacier ice and terrestrial haul-outs in the Kenai Fjords, Alaska. Marine Mammal Science 34:616–644.

Hoover-Miller, A., S. Atkinson, S. Conlon, J. Prewitt, and P. Armato. 2011. Persistent decline in abundance of harbor seals *Phoca vitulina richardsi* over three decades in Aialik Bay, an Alaskan tidewater glacial fjord. Marine Ecology Progress Series 424:259–271.

Huber, H. R., S. J. Jeffries, R. F. Brown, R. L. Delong, and G. Vanblaricom. 2001. Correcting aerial survey counts of harbor Seals (*Phoca vitulina richardsi*) in Washington and Oregon. Marine Mammal Science 17:276–293.

Hueffer, K., D. Holcomb, L. R. Ballweber, S. M. Gende, G. Blundell, and T. M. O'Hara. 2011. Serologic surveillance of pathogens in a declining harbor seal (*Phoca vitulina*) population in Glacier Bay National Park, Alaska, USA and a reference site. Journal of Wildlife Diseases 47:984–988.

Jansen, J. K., J. L. Bengtson, P. L. Boveng, S. P. Dahle, and J. M. Ver Hoef. 2006. Disturbance of harbor seals by cruise ships in Disenchantment Bay, Alaska: an investigation at three spatial and temporal Scales. Technical Report, AFSC Processed Report 2006–02, Alaska Fisheries Science Center, National Marine Fisheries Service, Department of Commerce.

Jansen, J. K., P. L. Boveng, S. P. Dahle, and J. L. Bengtson. 2010. Reaction of harbor seals to cruise ships. Journal of Wildlife Management 74:1186–1194.

Jansen, J. K., P. L. Boveng, J. M. Ver Hoef, S. P. Dahle, and J. L. Bengtson. 2015. Natural and human effects on harbor seal abundance and spatial distribution in an Alaskan glacial fjord. Marine Mammal Science 31:66–89.

Jemison, L. A., G. W. Pendleton, C. A. Wilson, and R. J. Small. 2006. Long-term trends in harbor seal numbers at Tugidak Island and Nanvak Bay, Alaska. Marine Mammal Science 22:339–360.

Kiszka, J. J., M. Heithaus, and A. Wirsing. 2015. Behavioural drivers of ecological roles and importance of marine mammals. Marine Ecology Progress Series 523:267–281.

Larsen, C. F., R. J. Motyka, A. A. Arendt, K. A. Echelmeyer, and P. E. Geissler. 2007. Glacier changes in Southeast Alaska and Northwest British Columbia and contribution to sea level rise. Journal of Geophysical Research: Earth Surface 112:F01007.

Lonergan, M., C. Duck, S. Moss, C. Morris, and D. Thompson. 2013. Rescaling of aerial survey data with information from small numbers of telemetry tags to estimate the size of a declining harbour seal population. Aquatic Conservation: Marine and Freshwater Ecosystems 23:1345–2144.

Mathews, E. A., and M. D. Adkison. 2010. The role of Steller sea lions in a large population decline of harbor seals. Marine Mammal Science 26:803–836.

Mathews, E. A., L. A. Jemison, G. W. Pendleton, K. M. Blejwas, K. W. Hood, and K. L. Raum-Suryan. 2016. Haul-out patterns and effects of vessel disturbance on harbor seals (*Phoca vitulina*) on glacial ice in Tracy Arm, Alaska. Fishery Bulletin 114:186–202.

Mathews, E. A., and B. P. Kelly. 1996. Extreme temporal variation in harbor seal (*Phoca vitulina richardsi*) numbers in Glacier Bay, a glacial fjord in Southeast Alaska. Marine Mammal Science 12:483–489.

Mathews, E. A., and G. W. Pendleton. 2006. Declines in harbor seal (*Phoca vitulina*) numbers in Glacier Bay National Park, Alaska, 1992–2002. Marine Mammal Science 22:167–189.

Mathews, E. A., W. L. Perryman, and L. B. Dzinich. 1997. Use of high-resolution, medium format aerial photography for monitoring harbor seal abundance at glacial ice haulouts. Technical Report, available from Glacier Bay National Park, PO Box 140, Gustavus, Alaska 99826.

McNabb, R. W., and R. Hock. 2014. Alaska tidewater glacier terminus positions, 1948–2012. Journal of Geophysical Research: Earth Surface 119:153–167.

McNabb, R. W., R. Hock, and M. Huss. 2015. Variations in Alaska tidewater glacier frontal ablation, 1985–2013. Journal of Geophysical Research: Earth Surface 120:120–136.

McNabb, R. W., J. N. Womble, A. Prakash, R. Gens, and C. E. Haselwimmer. 2016. Quantification and analysis of icebergs in a tidewater glacier fjord using an object-based approach. PLOS ONE 11:e0164444.

Miller, A. J., D. R. Cayan, T. P. Barnett, N. E. Graham, and J. M. Oberhuber. 1994. The 1976–77 climate shift of the Pacific Ocean. Oceanography 7:21–26.

Moreland, E. E., M. F. Cameron, R. P. Angliss, and P. L. Boveng. 2015. Evaluation of a ship-based unoccupied aircraft system (UAS) for surveys of spotted and ribbon seals in the Bering sea pack ice. Journal of Unmanned Vehicle Systems 3:114–122.

Ospina, R., and S. L. P. Ferrari. 2010. Inflated beta distributions. Statistical Papers 51:111–126.

Ospina, R., and S. L. P. Ferrari. 2012. A general class of zero-or-one inflated beta regression models. Computational Statistics and Data Analysis 56:1609–1623.

Pitcher, K. W. 1990. Major decline in number of harbor seals, *Phoca vitulina richardsi*, on Tugidak Island, Gulf of Alaska. Marine Mammal Science 6:121–134.

R Core Team. 2017. R: A language and environment for statistical computing. R Foundation for Statistical Computing, Vienna, Austria.

Seymour, A. C., J. Dale, M. Hammill, P. N. Halpin, and D. W. Johnston. 2017. Automated detection and enumeration of marine wildlife using unmanned aircraft systems (UAS) and thermal imagery. Scientific Reports 7:1–10.

Simpkins, M. A., D. E. Withrow, J. C. Cesarone, and P. L. Boveng. 2003. Stability in the proportion of harbor seals hauled out under locally ideal conditions. Marine Mammal Science 19:791–805.

Smithson, M., and J. Verkuilen. 2006. A better lemon squeezer? maximum-likelihood regression with beta-distributed dependent variables. Psychological Methods 11:54–71.

Strasburger, W., J. H. Moss, K. A. Siwicke, and E. M. Yasumiishi. 2018. Results from the eastern Gulf of Alaska ecosystem assessment, July through August 2016. U.S. Department of Commerce, NOAA Tech. Memo. NMFS-AFSC-363, 90p.

Streveler, G. 1979. Distribution, population ecology and impact susceptibility of harbor seals in Glacier Bay, Alaska. Technical Report, available from Glacier Bay National Park and Preserve, P.O. Box 140, Gustavus, Alaska 99826.

Sweeney, K. L., V. T. Helker, W. L. Perryman, D. J. LeRoi, L. W. Fritz, T. S. Gelatt, and R. P. Angliss. 2015. Flying beneath the clouds at the edge of the world: Using a hexacopter to supplement abundance surveys of Steller sea lions (*Eumetopias jubatus*) in Alaska. Journal of Unmanned Vehicle Systems 4:70–81.

Taylor, B. L., M. Martinez, T. Gerrodette, J. Barlow, and Y. N. Hrovat. 2007. Lessons from monitoring trends in abundance of marine mammals. Marine Mammal Science 23:157–175.

Taylor, B. L., P. R. Wade, D. P. De Master, and J. Barlow. 2000. Incorporating uncertainty into management models for marine mammals. Conservation Biology 14:1243–1252.

Trenberth, K. E., and J. W. Hurrell. 1994. Decadal atmosphere-ocean variations in the Pacific. Climate Dynamics 9:303–319.

Udevitz, M. S., J. R. Gilbert, and G. A. Fedoseev. 2001. Comparison of methods used to estimate numbers of walruses on sea ice. Marine Mammal Science 173:601–616.

Ver Hoef, J. M., and J. K. Jansen. 2015. Estimating abundance from counts in large data sets of irregularly-spaced plots using spatial basis functions. Journal of Agricultural, Biological, and Environmental Statistics 20:1–27.

Williams, P. J., M. B. Hooten, J. N. Womble, G. G. Esslinger, M. R. Bower, and T. J. Hefley. 2017. An integrated data model to estimate spatiotemporal occupancy, abundance, and colonization dynamics. Ecology 98:328–336.

Womble, J. N., G. M. Blundell, S. M. Gende, M. Horning, M. F. Sigler, and D. J. Csepp. 2014. Linking marine predator diving behavior to local prey fields in contrasting habitats in a subarctic glacial fjord. Marine Biology 1616:1361–1374.

Womble, J. N., and S. M. Gende. 2013. Post-breeding season migrations of a top predator, the harbor seal (*Phoca vitulina richardii*), from a marine protected area in Alaska. PLOS ONE 8:e55386.

Womble, J. N., G. W. Pendleton, E. A. Mathews, G. M. Blundell, N. M. Bool, and S. M. Gende. 2010. Harbor seal (*Phoca vitulina richardii*) decline continues in the rapidly changing landscape of Glacier Bay National Park, Alaska 1992–2008. Marine Mammal Science 26:686–697.

Young, C., S. M. Gende, and J. T. Harvey. 2014. Effects of vessels on harbor seals in Glacier Bay National Park. Tourism in Marine Environments 10:5–20.

Supporting Information

Additional Supporting Information may be found online at: http://onlinelibrary.wiley.com/doi/10.1002/ecs2.3111/full